2021 18th International Conference on Electrical Engineering, Computing Science and Automatic Control (CCE). Mexico City, Mexico. November 10-12, 2021

Synthesis, characterization, and structure computational calculations of the oxycalcogenide LaCuOSe for thermoelectric applications.

1st J.A. Melchor-Robles
Doctorado Nanociencias y Nanotecnologías, CINVESTAV-IPN ,México. Avenida Instituto Politécnico Nacional 2508, Col.San Pedro Zacatenco, Alcaldía Gustavo A. Madero,Cp. 07360, CDMX.
jairmelchor@gmail.com

2nd T.G.Díaz-Rodríguez
Programa de Doctorado en Ciencias en la especialidad de Ingeniería Eléctrica, CINVESTAV-IPN ,México. Avenida Instituto Politécnico Nacional 2508, Col.San Pedro Zacatenco, Alcaldía Gustavo A. Madero,Cp. 07360, CDMX. Estancias Posdoctorales Vinculadas al Fortalecimiento de la Calidad del Posgrado Nacional por CONACYT convocatoria 2020 (1).
tgdiazr@gmail.com

3rd Jacobo Martínez-Reyes
Programa de Doctorado Nanociencias y Nanotecnologías, CINVESTAV-IPN ,México. Avenida Instituto Politécnico Nacional 2508, Col.San Pedro Zacatenco, Alcaldía Gustavo A. Madero,Cp. 07360, CDMX. Estancias Posdoctorales Vinculadas al Fortalecimiento de la Calidad del Posgrado Nacional por CONACYT convocatoria 2020 (1).
jacobomartinezreyes@gmail.com

4th A. Maldonado-Álvarez
Departamento de Ingeniería Eléctrica SEES. CINVESTAV-IPN,México. Avenida Instituto Politécnico Nacional 2508,Col.San Pedro Zacatenco, Alcaldía Gustavo A. Madero, Cp. 07360, CDMX

5th María de la Luz Olvera-Amador
Departamento de Ingeniería Eléctrica SEES. CINVESTAV-IPN,México. Avenida Instituto Politécnico Nacional 2508,Col.San Pedro Zacatenco, Alcaldía Gustavo A. Madero, Cp. 07360, CDMX.
molvera@cinvestav.mx

***Abstract*—The synthesis of the LaCuOSe compound was carried ou via solid-state reaction. The synthesized samples were analyzed by X-ray diffraction, scanning electron microscopy, and RAMAN spectroscopy. The LaCuOSe compound shows the existence of traces of the La2Cu (SeO3) 4 phase. Computational calculations were performed to determine the electronic structure and estimate the band gap energy using the Density Functional Theory, DFT, using the screened hybrid functional HSE06.**

Keywords—LaCOSe, p-type semiconductors, oxycalcogenides, thermoelectric materials.

I. INTRODUCTION

The energy demand by 2040 faces a dual challenge represented by the need to produce more energy to support the global economic growth and boost a faster transition to a lower hydrocarbon consumption [1]. Based on the current and future energy demand, not only new energy sources are required, but also the efficient use of traditional energy sources to reduce energy losses [2].

A technological tool to convert residual heat from energy production processes into usable electricity is through the use of thermoelectric devices based on solid state electronics (DTE). DTEs are devices that use temperature gradients to generate electricity due to the potential difference generated, which is due to the movement of the electrons from the hot end of the material to the cold end. The thermoelectric process only occurs in certain materials, mainly in semiconductors. This physical phenomenon is known as the thermoelectric effect or thermoelectricity and includes three different effects, Seebeck effect, the Peltier effect and the Thomson effect [3-9].

The fundamental problem in designing efficient thermoelectric materials is that they need to be very good at transmitting electricity, but not heat. The performance of a thermoelectric material at a temperature T is determined by its Figure of Merit, ZT, which is a dimensionless parameter:

$$ZT = S2\sigma T/K \quad (1)$$

Where S is the Seebeck coefficient, σ the electrical conductivity and K is the thermal conductivity.

Among the elemental materials that present a high ZT value are Se, Te, Si and Ge. In the search to increase the efficiency of DTEs, in recent years, efforts have focused on the study of new composite materials. In this respect, the systems of interest are chalcogenides and polycrystalline oxycalcogenides, which have good chemical and thermal stability compared to metallic alloys.

Oxycalcogenides, LnCuOCh (Ln = lanthanide, Ch = chalcogen) are structurally formed by alternating stacks of an ionic oxide layer $(Ln_2O_2)^{2+}$ and a covalent chalcogenide layer $(Cu_2Ch_2)^{2-}$ along the [001] direction, which leads to interesting electronic properties and can be modulated by chemical substitution in both layers. This layered structure is the reason for the wide bandwidth presented by these materials, ˜ 3.2 eV [11-16].

One of the oxycalcogenides most studied is one containing Cu and Se in combination with lanthanum, La, which has an atomic structure built from layers of polyhedral units. Ueda´s et al research report that oxycalcogenides, LnCuOCh, are materials composed of mix anions, that is, divalent oxygen and chalcogen anions [17].

Although each cation in oxycalcogenides is generally coordinated by oxygen and chalcogen anions, the situation in LnCuOCh oxycalcogenides differs due to their layered crystalline structure; Cu ions are coordinated only by chalcogen anions that influence the anomalous contraction of the volume of the unit cell in monophasic phase. Many works have been developed on oxycalcogenides. The oxyselenide system, $La_{1-x}Sr_xCuOSe$, showed a degenerate p-type electrical conductivity due to the introduction of Sr [19]. A similar situation occurs in the oxysulfides, LaCuOS, [20,21], where the incorporation of S leads to a high optical transmission (⩾70%) in the visible and near infrared region and a band gap energy of approximately 3.1 eV with positive Seebeck coefficients, indicating that the dominant electrical conduction in these materials is p-type.

On the other hand, Bsnnikov identified that the replacement of metal atoms and chalcogens in LaMChO systems (M = Cu, Ag, and Ch = S, Se) lead to an anisotropic deformation of the crystal structure and a decrease of the band gap energy in semiconductors with minimal direct transitions between bands derived from the mixture of ionic and covalent contributions [22].

Regarding the compound $La_2Cu(SeO_3)_4$, Harrison et al. reported results on this; they observed that lanthanum cations are crystallochemically linked with copper and selenium in combination with oxygen to promote states of stable oxidation, identifying that copper has a degree of flexibility in its coordination preference, in contrast, selenium (IV) always shows a pyramidal geometry like selenite $[SeO_3^{2-}]$, revealing the presence of different phases [23].

978-1-6754-029-9/21/$31.00 ©2021 IEEE

In this work the synthesis of the LaCuOSe system by reaction in solid state is reported, as well as its microstructural characterization and the determination of the electronic properties of oxycalcogenides for their potential application in photocatalysis and thermoelectrics.

II. EXPERIMENTAL METHODOLOGY

A. *Synthesis process*

The polycrystalline system LaCuOSe was synthesized from pure CuO powders (99.9999% powder, fom Sigma Aldrich), Se (99.999% powder, from Sigma Aldrich), and La_2O_3 (99.999% powder, from Sigma Aldrich) in stoichiometric ratio. The precursors were first mixed, and then grounded in an agate mortar by uniaxial pressure to break up the granules. The precursor powders were weighed in the appropriate amount to obtain a total mass of 4g. The traditional "solid-state reaction" method was used to synthesize the system LaCuOSe [8,9]. Subsequently, the powder mixture was mechanically pressed into a 7 mm diameter stainless steel die, at room temperature with a pressure that varied from 10 to 0 Ton for 10 minutes; the pellets resulted mechanically stable.

B. *Characterization*

B.1 X-ray diffraction

To analyze the crystalline structure of the system under study, a PANalytical model X-Pert Pro diffractometer was employed, using the CuKα emission (λ = 1.54178 Å), at a voltage of 45 KV and a current of 40 mA with an angle scanning from 10 to 120 °, and a speed of 0.02 ° degrees per minute. In addition, for the analysis and assignment of the presented phases, the Match software from Crystal Impact, DIFFRAC plus EVA from BRUCKER Company and the database of the International Center for Diffraction Data, ICDD, were used.

B.2 Scanning Electron Microscopy and EDX analysis

The morphology of the systems was characterized by high resolution scanning electron microscopy in a JEOL JSM-7401F equipment, the voltage used to analyze the sample was in the range of 18 to 25 kV, with a current of 15 nA. The elemental chemical analysis of the sample was carried out by Energy Dispersive X-rays (EDX).

B.3 Raman spectroscopy

The identification of the low frequency modes, such as vibratory and rotary of the LaCuOSe system were obtained by means of a Horiba Jobin-Yvon Olympus BX40 equipment, equipped with a 100 W halogen lamp and a high resolution video camera for the sample positioning. The equipment uses a 633 nm laser with a 250 mW output with a 10 10m spot size and a 100X objective lens, using an exposure time of 60 s and a laser power of 5 nW. All spectra were measured with a resolution of 4 cm, from 100 to 3500 cm^{-1}, and 1 cm^{-1} pixel resolution. The spectra analysis was developed by the PerkinElmer Spectrum software

B.3 Electronic structure calculation

The computational calculations of the electronic structure were performed with the Density Functional Theory (DFT), as implemented with the FHI-AIMS computational code [10]. The screened hybrid functional developed by Heyd, Scuzeria, and Ernzerhof (HSE06) was used [11]. The structural optimizations of the LaCuOSe in bulk, were implemented with the functional HSE06 [12]. For the integration in the first Brillouin zone, a special k-point meshing was used under the Monkhrost-Pack scheme [12]. The convergence was achieved with respect to the k-point density sampling, 6x6x6, and the plane wave energy cutoff, 1e-6. The calculations converged for the forces on all the lower atoms of $1x10^{-2}$ eV / Å. The calculations were performed using atomic base functions, with a tier1 base established for all atoms.

III. RESULTS AND DISCUSSION

A. *X-ray diffraction*

The samples synthesized by solid-state reaction presented good correspondence with the LaCuOSe diffraction pattern, corresponding to the ICCD-PDF 49-1221 [14] card, however, traces of the $La_2Cu(SeO_3)_4$ phase (Lanthanum Copper Selenate) with monoclinic structure, identified with the card ICDD-PDF 88-0654 [7], were also identified. Figure 1 shows a typical diffractogram of the synthesized samples, where most of the peaks corresponding to the two mentioned phases have been detected. Additionally, the patterns of diffraction lines corresponding to the PDFs (Powder *Diffraction* Files) of the database of the International Center for Diffraction Data, ICDD (Figs. 1 A and B), and the unit cells modeled for the tetragonal structure of LaCuOSe and the monoclinic of $La_2Cu(SeO_3)_4$ are shown in the same figure. From the experimental diffractogram, the domain of the phase of interest, LaCuOSe, over the $La_2Cu(SeO_3)_4$ phase is evident; nevertheless regarding this, more experimental work is necessary to achieve the total obtaining of the LaCuOSe phase. It is worthy of noting that some diffraction peaks corresponding to the precursors were also present in the spectra, Se, CuO and La_2O_3.

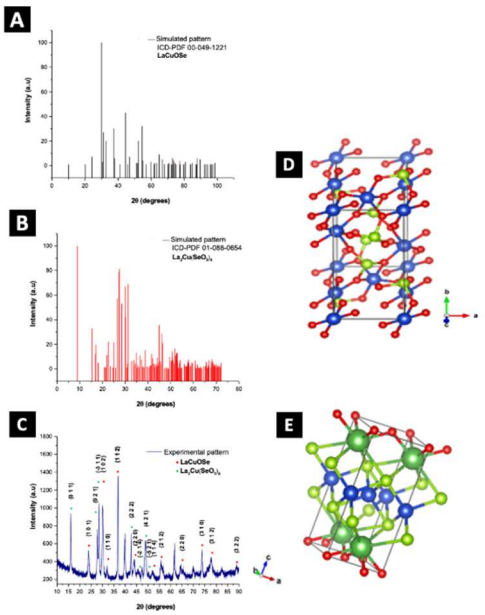

Fig. 1. A) Diffraction pattern of LaCuOSe phase, B) Diffraction pattern of $La_2Cu(SeO_3)_4$ phase, C) Diffraction pattern of synthesized LaCuOSe system, D) Atomic arrangement of the tetragonal structure of LaCuOSe, E) Atomic arrangement of the monoclinic structure of $La_2Cu(SeO_3)_4$.

Table 1 presents a resume of the crystallographic parameters of the two phases present in the synthesized system, LaCuSeO and $La_2Cu(SeO_3)_4$.

On the other hand, the structure calculated for the $La_2Cu(SeO_3)_4$ phase shown in Figure 1E, described by Harrison et al [15], presents selenium (IV) with a pyramidal coordination geometry, and the selenite group $[SeO_3^{2-}]$ as a flexible and stable element in the formation of polyhedral units. The intervention of La cations complete the structure of the $La_2Cu(SeO_3)_4$ phase due to their high coordination with oxygen [16]. Table 1 presents a summary of the crystallographic parameters of the two phases present in the synthesized system, LaCuSeO and $La_2Cu(SeO_3)_4$.

Table 1. Crystallographic parameters of the systems LaCuSeO and $La_2Cu(SeO_3)_4$

FORMULA	***ICDD-PDF CARD***	***CRYSTALLINE STRUCTURE (QUALITY DIFFRACTIONS PATTERN)***	***LATTICE PARAMETER***	***Space Group***	***DETERMINATION MECHANISM***
LaCuSeO	49-1221	Tetragonal (*)	a=4.065 b=Nd c=8.793 β=Nd	P4/nmm (129)	Theoretical-Calculated
$La_2Cu(SeO_3)_4$	88-0654	Monoclinic (C)	a=10.51 b=7.136 c=8.431 β=110.61	P21/c (14)	Experimental-diffractometry

The monoclinic structure of the $La_2Cu(SeO_3)_4$ system is due to the contributions of elemental powders in the synthesis process and to the influence of La that normally crystallizes in an orthorhombic system (Pnma, space group), but being surrounded by chalcogen $[SeO_3^{2-}]$, its structure is strongly influenced by Se^{6+} cations and the species lead to a pyramidal coordination. There is also controversy over the coordination number of O with La. The La atom would be coordinated by eight O atoms, while Rice and

Robinson state that La exhibits an irregular coordination by nine O atoms instead of 8 [18].

The LaCuOSe phase presents a primitive structure with a space group P4/nmm(129) and a point group 4/mmm, resulting in a tetragonal crystal system. The structure is two-dimensional and consists of a layer of ionic oxide $(La_2O_2)^{2+}$ and a layer of covalent chalcogenide $(Cu_2Se_2)^{2-}$ along the [001] direction. In the Cu-Se layer, Cu^{1+} is attached to four equivalent Se^{2-} atoms to form a mixture of $CuSe_4$ tetrahedra at the corner and edge they share. In the La-O sheet, the La^{3+} is with four equivalent O atoms and the O^{2-} is attached to four equivalent La^{3+} atoms to form a mixture of tetrahedra.

Copper oxide (CuO) is generated in situ from cuprous selenide (Cu_2Se) under oxygen evolution reaction conditions. The incorporation of La into the CuO lattice reduces crystallinity due to the variation of ionic radii. This change in crystallinity may also be due to the partial occupation of vacancies by La ions, causing deformations in the lattice [19].

B. Scanning electron microscopy and EDX

The LaCuSe system presents a characteristic morphology of an alloying process (Figure 2A), due to the presence of transition zones at the interfaces of the individual compounds. The local compositional analysis performed by EDX shows the dispersed presence of the elements La, Cu and Se, as well as a prominent oxygen signal (Figure 2B and 2C). However, the quantitative composition yields values that are not representative of the phases observed by X-ray analysis.

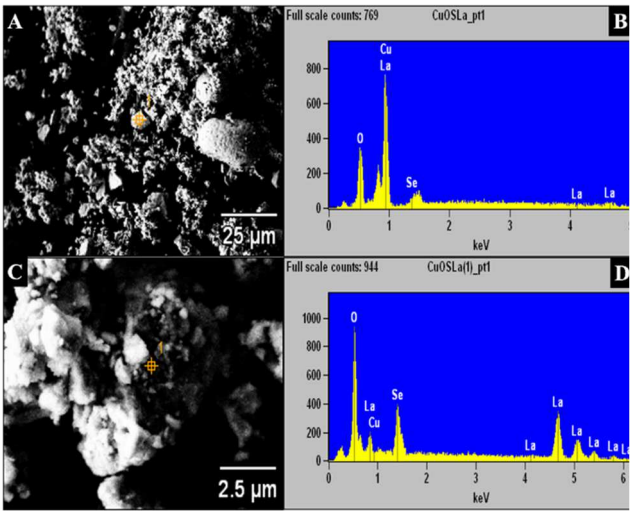

Fig. 2. A,B) SEM images of the system LaCuOSe in different zones. C,D) EDX spectra of punctual composition analysis of the LaCuOSe sample.

The qualitative information obtained from EDX and SEM images, validate the formation process of the LaCuOSe phase as well as its influence that has the concentration of lanthanum and oxygen for its conformation. Wickleder et al. reported that the concentration of the anions, La and O, present in the solid-state reaction are decisive in obtaining the LaCuOSe phase [20].

C. Raman spectroscopy

Figure 3 shows the Raman spectrum of the LaCuOSe system. In this, the characteristic peaks of the vibrational modes of the base elements of the systems detected in the X-ray analysis are observed, as well as areas of less resonance due to the presence of clusters and impurities of the phase derived by the presence of traces of $La_2Cu(SeO_3)_4$.

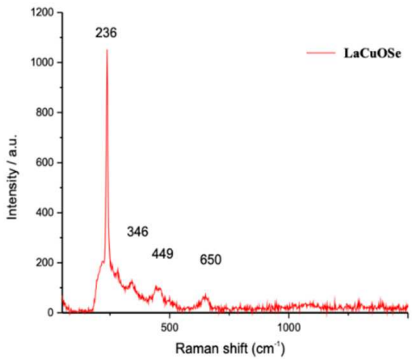

Fig 3. Raman spectrum of the LaCuOSe system.

The characteristic peak of Se, ~245 cm^{-1} (B2), are assigned due to the local heating of the sample that causes tension in the amorphous lattice, which induces an increase in the vibration force, therefore, in the modes vibratory changes to smaller wave numbers. Other peaks identified for selenium are 442 and 2193 cm^{-1}. The vibrational modes of La are observed at ~ 290 cm^{-1} (T1u), 350, 414, 616 cm^{-1} (T2g), 1080 cm^{-1} (Eg), CuO ~ 215 (Eu), 306 (Ag), 425, 500 (Eg), 653 cm^{-1} (Bg), 800, 1289 cm^{-1}. In the range of 400-500 cm^{-1}, two bands at ~447, 449 and 500 cm^{-1} with a high content of La_2O_3 are located.

D. Electronic structure calculation

The crystal structure of the LaCuOSe system (Figure 4A) is tetragonal of the ZrCuSiAs type, with a space group P4/nmm (129). This structure is formed by a stacking of $[La_2O_2]$ and $[Cu_2Se_2]$ along the c axis [21].

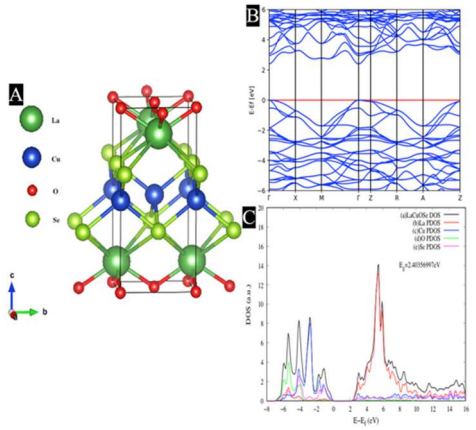

Fig 4. Computational calculations of the LaCuOSe system. A) Electronic structure, B) Two-dimensional electronic band structure, C) Density of states.

Figure 4B shows the electronic band structure of LaCuOSe; which was calculated along a highly symmetrical trajectory, in the first Brillouin zone. In this case, the minimum conduction band (CBM) is at point Γ, and the minimum valence band (VBM) is at Γ; the CBM and VBM are at the same point. It can be seen that LaCuOSe phase has a direct band gap. The energy band gap calculated with the HSE06 functional for LaCuOSe is 2.5 eV. The calculated value agrees with the experimentally estimated energy band gap of 2.8 eV [22-26].

Regarding the total and partial density of states for LaCuOSe (Figure 1C), the valence bands consist of two parts: the first one part is located at lower energies, which are mainly the O-2 states. The medium valence bands are dominated by the Cu and Se-4s states. The strong contributions to the upper conduction bands come from the La-5d states. The edge of the conduction band is mainly described by La, Cu, O, and Se, with the same proportion.

The total of the crystalline electronic states is predominantly determined by La, O and Cu, this characteristic qualitatively explains how the metallic atoms compete with the non-metallic atoms for the electrons provided by the cations and consequently they will behave as anions.

Ueda estimate energy band gap of LaCuOSe ~1.48 to 2.82 eV, The valence bands consist of two parts: the first part is located at lower energies, which is mainly the O-2s states. The middle valence bands are dominated by Cu and Se-4s states. The strong contributions to the upper valence bands are

coming from the La-5d states. The conduction band edge is described mainly by La, and Cu, and Se, with the same proportion [26,27].

We comment that one of the possibilities of the underestimation of the calculation of the theoretical band gap by 0.300 eV of LaCuOSe, is due to that the calculation was carried out with the FHI-AIMS code, with the functional developed by Heyd , Scuzeria, and Ernzerhof (HSE06), but without included the Van de Waals interaction (vdW) in the methodology used. As reported by Wang et. al.[28], this interaction has some influence on the LaCuOSe and BiCuOSe type systems.Nevertheless, it is shown that the band gap obtained by DFT method without vdW correction are all in reasonable agreement with experimental values[29].

IV. Conclusion

The synthesized LaCuOSe system presented a tetragonal phase combined with traces of the $La_2Cu(SeO_3)_4$ phase, which was corroborated by X-ray diffraction. The morphological analysis shows the typical characteristics of an alloy due to the evident intergranular transition zones. The Raman characterization confirmed some vibration modes of the LaCuOSe system. The energy bandgap calculated from HSE06 of the LaCuOSe system is 2.5 eV and fits well with the experimentally estimated energy band gap, 2.8 eV.

The synthesis as well as the microstructural characterization and simulation of the electronic structure of the chalcogenide oxide LaCuOSe allows suggesting it as a promising material for thermoelectric applications.

V. AKNOWLEDGMENTS

Jacobo Martínez-Reyes and T.G. Díaz-Rodríguez thank the economical support received from “Estancias Posdoctorales Vinculadas al Fortalecimiento de la Calidad del Posgrado Nacional por CONACYT, convocatoria 2020 (1)”.

The technical support of M.A- Luna-Arias and A. Tavira-Fuentes is grateful.

References

[1] Erdiwansyah, Mahidin, Mamat R., Sani M.S.M., Khoerunnisa Fitri, Kadarohman Asep. Target and demand for renewable energy across 10 ASEAN countries by 2040. The Electricity Journal (2019), 32,10, 106670. https://doi.org/10.1016/j.tej.2019.106670

[2] Ueda K., Takafuji K., Hosono H.Preparation and crystal structure analysis of CeCuOS. Journal of Solid State Chemistry (2003),170,1,182–187. https://doi.org/10.1016/S0022-4596(02)00061-0

[3] Yasukawa M. Thermoelectric properties of layered oxyselenides La1−xSrxCuOSeLa1−xSrxCuOSe (x=0(x=0 to 0.2). Journal of Applied Physics (2004),95,7,3594-3597. https://doi.org/10.1063/1.1646438

[4] Ueda K., Hirose S., Kawazoe H., Hosono H. Transparent p-type semiconductor: LaCuOS layered oxysulfide. Applied Physics Letters. (2000),77, 2701- 2703.https://doi.org/10.1063/1.1319507

[5] Hiramatsu H, Ueda K., Ohta H., Orita M., Hirano M., Hosono H. Heteroepitaxial growth of a wide-gap p-type semiconductor, LaCuOS. Appllied Physics Letters. (202),81,598. https://doi.org/10.1063/1.1494853

[6] Bannikov V.V., Ivanovskii A.L.Structural, electronic properties and inter-atomic bonding in layered chalcogenide oxides LaMChO (where M=Cu,Ag, and Ch=S,Se) from FLAPW-GGA calculations. Solid State Sciences (2012),14,89-93. https://doi.org/10.1016/j.solidstatesciences.2011.10.022

[7] Harrison W.T.A., Zhang Z. (1997) Synthesis and crystal structure of $La_2Cu(SeO_3)_4$. Journal of Solid State Chemistry 133,2,572-575. ICD-PDF 88-065. https://doi.org/10.1006/jssc.1997.7515

[8] Hiramatsu H.,Ohta H.,Suzuki T.,Honjo C., Ikuhara Y.,Ueda K.,Kamiya T.,Hirano M.,Hosono H. Mechanism for heteroepitaxial growth of a wide-gap p-type semiconductor:LaCuOS by Reactive Solid-Phase Epitaxy.Crystal Growth & Design (2004),4,2,301-307. https://doi.org/10.1021/cg034163l

[9] Gamon J., Giaume D., Wallez G., Labégorre J-B., Lebedev O.I., Al Orabi R. Al Rahal, Haller S., Le Mercier T., Guilmeau E., Maignan A., Barboux P.. Substituting copper with silver in the BiMOCh layered Compounds (M=Cu or Ag; Ch=S,Se, or Te): Crystal, electronic structure, and optoelectronic properties. Chemistry of Materials (2018),30,2,549-558. https://doi.org/10.1021/acs.chemmater.7b04962

[10] Volker Blum, Ralf Gehrke, Felix Hanke, Paula Havu, Ville Havu, Xinguo Ren, Karsten Reuter, Matthias Scheffler, Ab initio molecular simulations with numeric atom-centered orbitals, Computer Physics Communications, Volume 180, Issue 11, 2009, Pages 2175-2196, ISSN 0010-4655, https://doi.org/10.1016/j.cpc.2009.06.022 .

[11] Heyd,Jochen and Scuseria,Gustavo E. and Ernzerhof,Matthias, Hybrid functionals based on a screened Coulomb potential, The Journal of Chemical Physics (2003),118,18,8207—8215. doi:10.1063/1.1564060.

[12] Monkhorst, Hendrik J. and Pack, James D, Special points for Brillouin-zone integrations, Phys. Rev. B, 1976, Volume 13, pages 5188—5192, doi: https://link.aps.org/doi/10.1103/PhysRevB.13.5188

[13] Hiramatsu H.,Ueda K.,Ohta H.,Orita M.,Hirano M.,Hosono H. Heteroepitaxial growth of a wide-gap p-type semiconductor, LaCuOS.Applied Physics Letters (2002), 81, 598. https://doi.org/10.1063/1.1494853

[14] Abakumov,A.Antipov E. Chemical Dept.Moscow State Univ. Russia, ICDD Grant-in-Aid (1997)ICD-PDF 49-1221.

[15] William T.A. Harrison, Zhanghua Zhang. Synthesis and Crystal Structure of $La_2Cu(SeO_3)_4$. Journal of Solid State Chemistry (1997),133,2,572-575. https://doi.org/10.1006/jssc.1997.7515

[16] R. Morris, W. T. A. Harrison, G. D. Stucky, A. K. Cheetham. The synthesis and crystal structure of $LaHSe_2O_6$, a layered anhydrous selenite.Acta Crystallographica Section C (1992). C48, 1182-1185. https://doi.org/10.1107/S0108270191014300

[17] Brusset H.,Maduale-Aubry F.,Mahe R., Boursier C., C.R. Acad. Sci. Paris, Ser. C 273 (1971) 455

[18] Rice C.E., Robinson W., Lanthanum orthovanadate.Acta Crystallographica Section B. B32 (1976), 2232-2233. https://doi.org/10.1107/S0567740876007450

[19] Vimala Devi L., Sellaiyan S.,Sankar S.,Sivaji K..Structural and optical investigation of combustion derived La doped copper oxide nanocrystallites. Materials Research Express (2018),5,024002. https://doi.org/10.1088/2053-1591/aaa7a3

[20] Wickleder M.S. Inorganic Lanthanide compounds with complex anion. Chemical Reviews.(2002),102,6,2011-2088. https://doi.org/10.1021/cr010308o

[21] Bannikov, V.V., Shein, I.R. & Ivanovskii, A.L. Impurity-Induced Magnetization of Layered Semiconductor LaCuSeO as Predicted from First-Principles Calculations. Journal of Superconductivity and Novel Magnetism (2012), 25, 1509–1513. https://doi.org/10.1007/s10948-012-1415-6

[22] Ueda,Kazushige and Hosono,Hideo, Band gap engineering, band edge emission, and p-type conductivity in wide-gap LaCuOS1−xSex oxychalcogenides, Journal Journal of Applied Physics, (2002),91, 7,4768—4770, doi: 10.1063/1.1456240.

[23] Bannikov V.V.,Shein I.R. Anionic state of platinum-group metal atoms in a series of ternary and quaternary compound. Computational Condensed Matter (2020), 22,e00441. https://doi.org/10.1016/j.cocom.2019.e00441.

[24] Ueda K.,Hiramatsu H.,Ohta H.,Hirano M.,Kamiya T.,Hosono H. Single atomic layered quantum wells built in wide-gap semiconductors LnCuOCh (Ln=lanthanide,Ch=chalcogen). Physical Review B (2004), 69,155305. https://doi.org/10.1103/PhysRevB.69.155305

[25] Hiramatsu H.,Yanagi H.,Kamiya T.,Ueda K.,Hirano M.,Hosono H. Crystal structures,optoelectronic properties and electronic structures of layered oxychalcogenides McuOCh (M=Bi,La;Ch=S,Se,Te):Effects of electronic configurations of M3+ ions. Chemistry of Materials (2008),20,1,326-334. https://doi.org/10.1021/cm702303r

[26] Ueda K,Takafuhi K.,Yanagi H.,Kamiya T.,Hosono H., Hiramatsu H.,Hirano M.,Hamada N. Optoelectronic properties and electronic structure of YCuOSE. Journal of applied physics (2007),102,113714. https://doi.org/10.1063/1.2821763

[27] Ueda,Kazushige and Hosono,Hideo, Band gap engineering, band edge emission, and p-type conductivity in wide-gap LaCuOS1−xSex oxychalcogenides, Journal Journal of Applied Physics, 2002, Volume 91, Number 7, Pages 4768—4770, doi: 10.1063/1.1456240.

[28] Wang, N.Li,M.Xiao,H,Gao Z.,Liu Z.,Zu X.,Li S,Qiao L..Band degeneracy enhanced thermoelectric performance in layered oxyselenides by first-principles calculation. Npj Computational Materials (2021),7,18,1-13, doi:https://doi.org/10.1038/s41524-020-00476-3.

[29] Ohki,Y., Satoshi K., Yumiko T., Kouichi T., Yoshi T.,Kazuko S.Temperature dependence of the band edge emission of the wide gap

semiconductor (LaO)CuCh(Ch=S,Se,Te). 24th International Conference on Low Temperature Physics (2006),850,1,1309-1310, doi:https://doi.org/10.1063/1.2355188

978-1-6654-0029-9/21/$31.00 ©2021 IEEE